JOURNAL OF MAGNETIC RESONANCE 81, 474–483 (1989)

The Steady-State Signals in Short-Repetition-Time Sequences

MICHAEL L. GYNGELL

Max-Planck-Institut für biophysikalische Chemie, Postfach 2841, D-3400 Göttingen, Federal Republic of Germany

Received April 11, 1988; revised July 7, 1988

In the steady-state free precession sequence a regular sequence of phase-coherent radiofrequency pulses is applied with a repetition time shorter than the NMR relaxation times of the sample under investigation. The intensity of the resulting NMR signal has a complicated dependence on sequence repetition time and RF pulse angle, as well as dependence on the relaxation times. The purpose of this paper is to present a simple mathematical description of the SSFP NMR signals which may be used to accurately model SSFP experiments. Experimental verification of the model has been carried out on a 40 cm bore 2.35 T Bruker Medspec system. © 1989 Academic Press, Inc.

With the upsurge of interest in rapid scanning by the use of short sequence repetition times (*1–6*) there has been much discussion over signal behavior as a function of flip angle with a view to predicting the contrast capabilities of such methods (*7–9*). The use of repetition times shorter than the T_1 and T_2 relaxation times results in dynamic equilibrium in both the longitudinal and the transverse magnetizations in which the NMR signal and thus image contrast has a complicated dependence on T_1 and T_2. It has also been observed that image contrast is flip-angle dependent.

The steady-state free precession (SSFP) sequence (*10*) consists of an arbitrarily long string of phase-coherent radiofrequency pulses of the same flip angle applied with a constant and short repetition time, Fig. 1. It is possible to draw an analogy between two adjacent repetitions in the SSFP sequence and the Hahn spin-echo experiment (*5*). Each RF pulse is followed by a FID which is refocused by the following RF pulse to form a spin echo at the end of the next repetition interval. Each FID may be thought of as being entirely due to fresh longitudinal magnetization. And the ratio of the echo signal to the FID signal will be given by

$$S_{\text{echo}}/S_{\text{fid}} = \exp(-2T_R/T_2)\sin^2(\alpha/2). \quad [1]$$

Stimulated echo effects may also be taken into consideration by comparing a three-pulse experiment to SSFP. The first pulse excites a FID. The second pulse applied after a short delay generates longitudinal magnetization from the FID, and the third pulse applied after a further delay gives rise to a stimulated echo. Identification of three consecutive pulses in the SSFP sequence with the stimulated echo model shows that the simulated echo occurs at the same time as a subsequent RF pulse, which also coincides with the spin echo described above. The ratio of the stimulated echo component to the FID component is given by

0022-2364/89 $3.00

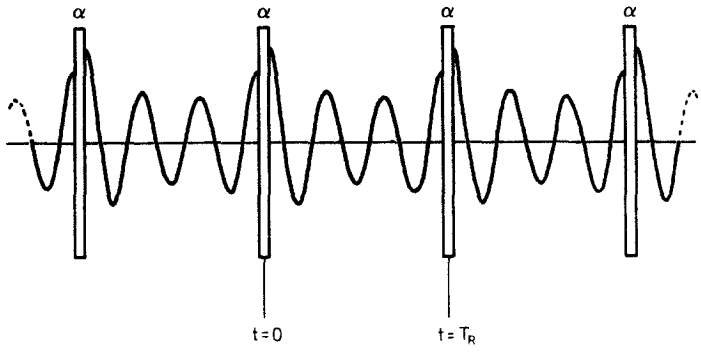

FIG. 1. Radiofrequency pulse sequence for the steady-state free precession sequence. It consists of a long string of phase-coherent RF pulses of the same pulse angle applied with a constant repetition time. In the steady state, the signal appearing between pulses is identical for all repetitions.

$$S_{ste}/S_{fid} = 0.5 \exp(-2T_R/T_2)\exp(-T_R/T_1)\sin^2(\alpha). \quad [2]$$

Obviously these two components have different flip-angle dependence and different T_1 dependence. This results in the complex flip-angle-dependent contrast observed in short-repetition-time NMR imaging experiments. The consideration of analogies with four or more pulses reveals further complexity in the signal response.

It is the purpose of this paper to present a simple mathematical description of the signals occurring in the SSFP sequence.

THEORETICAL CONSIDERATIONS

In the steady state the transverse components of the magnetization at a time $t = 0$ immediately after a RF pulse are given by (*11*)

$$M_x(0, \delta\omega) = QE_2(T_R)\sin(\alpha)\sin(\delta\omega T_R) \quad [3]$$

$$M_y(0, \delta\omega) = Q\sin(\alpha)(1 - E_2(T_R)\cos(\delta\omega T_R)), \quad [4]$$

where

$$Q = \frac{M_0(1 - E_1(T_R))}{p - q\cos(\delta\omega T_R)} \quad [5]$$

$$E_1(t) = \exp(-t/T_1) \quad [6]$$

$$E_2(t) = \exp(-t/T_2) \quad [7]$$

$$p = 1 - E_1(T_R)\cos(\alpha) - E_2(T_R)^2(E_1(T_R) - \cos(\alpha)) \quad [8]$$

$$q = E_2(T_R)(1 - E_1(T_R))(1 + \cos(\alpha)). \quad [9]$$

T_R is the sequence repetition time, $\delta\omega$ is the resonance offset of the isochromat under consideration, and α is the RF pulse angle. Of course the transverse magnetization may be expressed in complex notation, i.e.,

$$M_{xy}(0, \delta\omega) = M_y(0, \delta\omega) + jM_x(0, \delta\omega) \quad [10]$$

$$= Q\sin(\alpha)(1 - E_2(T_R)e^{-j\delta\omega T_R}) \quad [11]$$

and the evolution of M_{xy} during the subsequent repetition interval (*12*) will be given by

$$M_{xy}(t, \delta\omega) = M_{xy}(0, \delta\omega)E_2(t)e^{j\delta\omega t} \quad [12]$$

$$= Q\sin(\alpha)(E_2(t)e^{j\delta\omega t} - E_2(t + T_R)e^{j\delta\omega(t-T_R)}). \quad [13]$$

The transverse magnetization described by [13] clearly has two components; the first is the FID component which is "in-phase" at $t = 0$ and dephases as t increases and the second, the echo, which rephases at $t - T_R = 0$ at the end of each interval. The steady-state NMR signal may now be calculated by integrating [13] over all resonance offset frequencies, $\delta\omega$, within the sample,

$$S(t) = \int_{-\infty}^{+\infty} M_{xy}(t, \delta\omega)g(\delta\omega)d(\delta\omega), \quad [14]$$

where $g(\delta\omega)$ is the spin distribution function. Substitution of [13] into [14] gives

$$S(t) = \frac{M_0(1 - E_1(T_R))}{p}\sin(\alpha)\left\{E_2(t)\int_{-\infty}^{+\infty}\frac{g(\delta\omega)e^{j\delta\omega t}}{1 - (q/p)\cos(\delta\omega T_R)}d(\delta\omega)\right.$$

$$\left. - E_2(t + T_R)\int_{-\infty}^{+\infty}\frac{g(\delta\omega)e^{j\delta\omega(t-T_R)}}{1 - (q/p)\cos(\delta\omega T_R)}d(\delta\omega)\right\}. \quad [15]$$

The integration of [15] may be found in the Appendix. The amplitudes of the signals are given by

$$S_{fid} = \frac{M_0(1 - E_1(T_R))}{p}\sin(\alpha)(u - E_2(T_R)v) \quad [16]$$

$$S_{echo} = \frac{M_0(1 - E_1(T_R))}{p}\sin(\alpha)(E_2(2T_R)u - E_2(T_R)v). \quad [17]$$

The SSFP FID signal occurring at $t = 0$ is represented by [16] and the echo at $t = T_R$ by [17]. The terms u and v are given by

$$u = 1 + \sum_{m=1}^{\infty}\left(\frac{q}{2p}\right)^{2m}\binom{2m}{m} \quad [18]$$

$$v = \frac{1}{2}\sum_{m=1}^{\infty}\left(\frac{q}{2p}\right)^{2m-1}\binom{2m}{m}, \quad [19]$$

where p and q are given by [8] and [9], respectively. Since $|q| < |p|$ the summations converge (*13*). The summations in [18] and [19] imply that both the FID and the echo signals are composites of a number of coincident responses (*14*). This result may be understood in terms of higher-order coherences providing extra contributions to the principal FID and echo signals as suggested earlier. In a Carr–Purcell sequence a 90° pulse at $t = 0$ is followed by a string of 180° pulses at times $(2n - 1)\tau$, and a series of spin echoes arise at times $2n\tau$. The echo amplitudes describe the T_2 decay envelope of the sample (Fig. 2a). If the 180° refocusing pulses are imperfect (Fig. 2b) an additional set of secondary spin echoes and stimulated echoes will occur coinci-

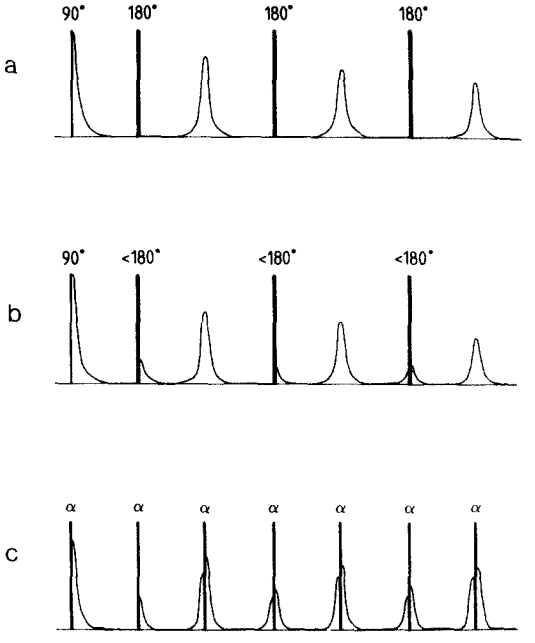

FIG. 2. Carr–Purcell to SSFP. The complexity of the SSFP signal may be understood in terms of the Carr–Purcell sequence. The use of imperfect refocusing pulses results in the generation of additional signals in the form of FIDs after each pulse and stimulated echoes and secondary echoes during each expected spin echo and each subsequent refocusing pulse. Replacing all the pulses by identical pulses of arbitrary flip angle and applying further pulses at the times of the expected spin echoes complete the picture with signals after and before each pulse being composites of spin echoes, stimulated echoes, and FIDs.

dentally with the expected echoes and refocusing RF pulses. The number of additional echoes increases rapidly as more refocusing pulses are applied. This also describes the low-angle RARE experiment (FLARE) (*15*) which employs imperfect refocusing pulses. Replacing the initial 90° pulse and the subsequent refocusing pulses by identical α pulses and applying further α pulses at times $2n\tau$ coincidentally with the primary spin echoes results in a SSFP-like sequence. Every pulse is followed by a FID-like signal and an echo-like signal reforms before each pulse, and both signals are composites of primary, secondary, and stimulated echoes (Fig. 2c).

The degree of phase coherence between successive repetitions is determined by T_2 and the RF flip angle and is defined by q given by [9] appearing in [18] and [19]. This term becomes negligible at repetition times long compared to T_2 where $E_2(T_R)$ is small and also at high flip angles where $(1 + \cos \alpha)$ becomes small. Thus higher-order and therefore longer-term coherences have increasing importance at lower flip angles as demonstrated by the fact that the summations in [18] and [19] tend to converge to within 0.01% in only 3 or 4 iterations for pulse angles above about 90° and that 50 to 100 iterations may be necessary for flip angles under 10°, depending on T_1 and T_2. This has been experimentally confirmed with a stopped SSFP sequence.

It has been suggested (*16*) that the ratio of echo to FID yields the T_2 relaxation time of the sample by the relation

$$\left|\frac{S_{\text{echo}}}{S_{\text{fid}}}\right| = \exp\left(\frac{-2T_R}{T_2}\right). \quad [20]$$

This result is not generally true but may be obtained from [16] and [17] only if the term q is negligible.

It is interesting to note that if the RF flip angle is chosen such that $\cos(\alpha) = \exp(-T_R/T_1)$ the SSFP FID signal is given by

$$S_{\text{fid}} = M_0 \sqrt{\frac{(1 - E_1)}{(1 + E_1)}} \quad [21]$$

and the echo signal is given by

$$S_{\text{echo}} = S_{\text{fid}}\left(E_2(2T_R) - (1 - E_2(2T_R)) \sum_{m=1}^{\infty} \left(\frac{E_2(2T_R)}{2}\right)^m \binom{2m}{m}\right). \quad [22]$$

Thus when Ernst angle excitation pulses are used the SSFP FID signal becomes independent of T_2 and the ratio of the SSFP echo to the SSFP FID signal becomes independent of T_1.

RESULTS

Experiments to test the validity of the equations for the SSFP FID and echo signals were performed using samples of water doped with manganese chloride on a 40 cm bore 2.35 T Bruker Medspec system. The T_1 and T_2 relaxation times of the samples were determined with an accuracy of 3% by inversion-recovery and spin-echo methods on the same machine. Two samples were used; the first had a concentration of 0.1 mmol, T_1 = 885 ms, and T_2 = 84 ms; and the second sample had a concentration of 0.5 mmol, T_1 = 278 ms, and T_2 = 21 ms.

The SSFP sequence consisted of a stream of 400 nonselective rectangular (hard) pulses, with a pulse repetition time of 20 ms. The pulse length was in the range of 1–60 μs. A weak gradient was applied between pulses to ensure separation of the FID and echo components. The signals were collected as a function of the SSFP pulse angle. For ease the signals were acquired at the end of the pulse stream and their amplitudes were determined from the Fourier transforms of the signals. In order to avoid problems of receiver saturation the SSFP FID had to be collected as a spin echo. This was achieved by applying a hard 180° pulse 10 ms after the pulse stream. The SSFP echo signal was collected without the 180° pulse. Thus both signals were acquired as full spin echoes.

The experimental results for the 0.5 and 0.1 mmol $MnCl_2$ solutions are shown in Figs. 3 and 4, respectively, with the FID data being scaled to compensate for the spin-echo acquisition. The solid lines refer to the theoretical results calculated using [14] and [15] from the measured T_1 and T_2 values. As it turns out the experimental data and theory are in excellent agreement.

Figures 5 and 6 show the ratios of the echo to the FID for the two samples; the solid lines refer to the theoretical results. Again there is good agreement between theory and practice. The T_2 for the samples may be estimated, using [20], from the plateau in the ratio of echo to the FID for pulse angles above 90°, giving T_2 estimates of 83

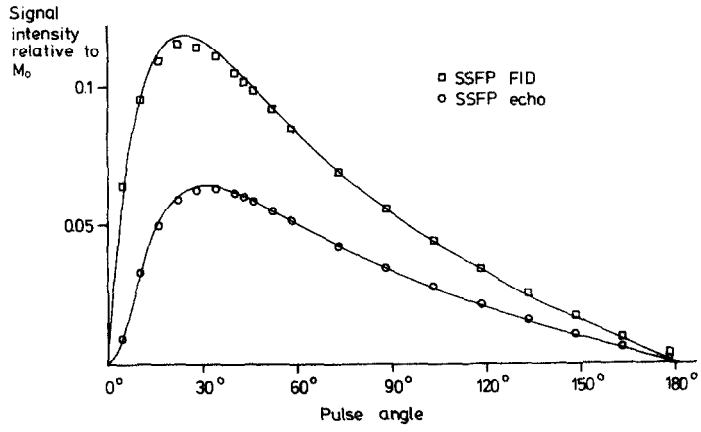

FIG. 3. A comparison of the experimental and theoretical signal levels of the SSFP FID and echo signals plotted as a function of pulse angle for 0.1 mM $MnCl_2$ solution (T_1 = 885 ms, T_2 = 84 ms, T_R = 20 ms). The solid lines were calculated on the basis of the measured T_1 and T_2 values for the sample determined from conventional inversion-recovery and spin-echo methods.

and 21 ms for the 0.1 and 0.5 mmol $MnCl_2$, respectively. This is in agreement with the T_2 values measured using the spin-echo method.

CONCLUSIONS

A mathematical description of the NMR signal in the steady-state free precession experiment has been obtained by integrating the well-known equations for the SSFP transverse magnetization with respect to resonance offset. This description was found to be in excellent agreement with experimental results. The signal is composed of two

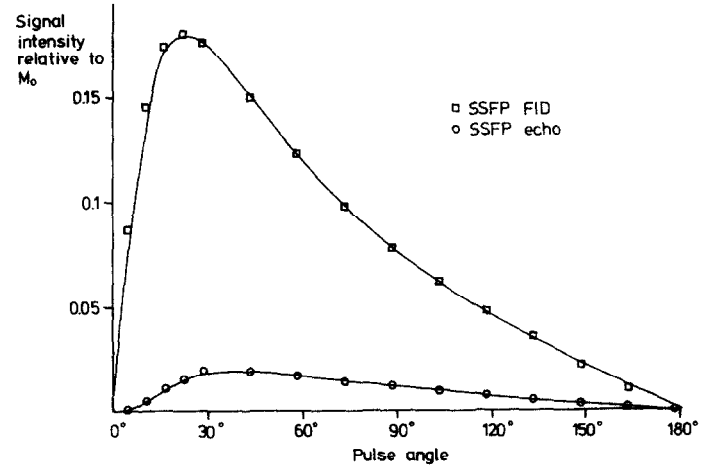

FIG. 4. A comparison of the experimental and theoretical signal levels of the SSFP FID and echo signals plotted as a function of pulse angles for 0.5 mM $MnCl_2$ solution (T_1 = 277 ms, T_2 = 21 ms, T_R = 20 ms). The solid lines were calculated on the basis of the measured T_1 and T_2 values for the sample determined from conventional inversion-recovery and spin-echo methods.

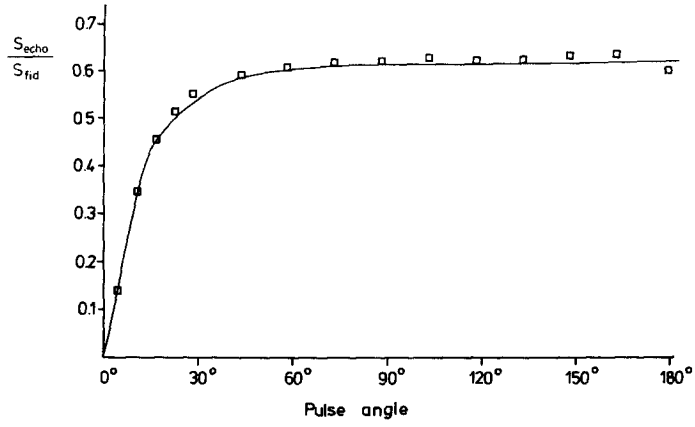

FIG. 5. A comparison of the experimental (□) and theoretical (solid line) pulse angle dependence of the ratio of SSFP echo to SSFP FID for 0.1 mM $MnCl_2$ solution (T_1 = 885 ms, T_2 = 84 ms, T_R = 20 ms).

distinct parts taking the form of a free induction signal [16] decaying away after each pulse and an echo signal [17] forming before each pulse. The two signals have a complex nature, being the resultants of many coincident coherent signals, such as FIDs, spin echoes, and stimulated echoes from previous repetitions, as indicated by the summations in [18] and [19]. The different flip-angle dependence of the various coincident signals combined with their different T_1 and T_2 dependence leads to the flip-angle-dependent contrast observed in short-repetition-time NMR imaging sequences.

The degree of phase coherence between successive repetitions is not only determined by the ratio of repetition time to T_2 but also by the flip angle. At high flip angles, above 90°, there is a rapid interchange of longitudinal magnetization and transverse magnetization due to the RF pulses, so that the phase coherence of the

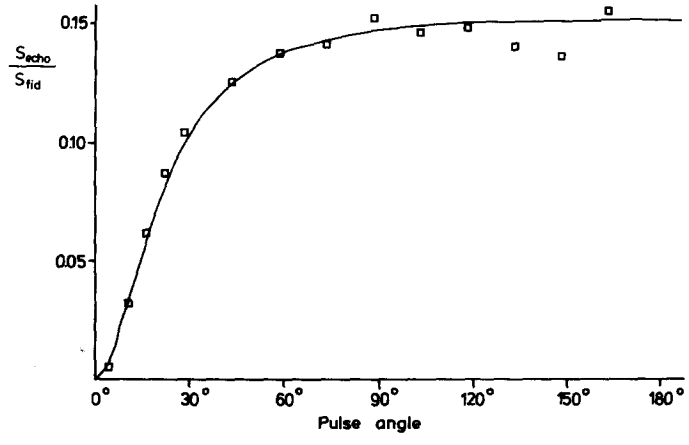

FIG. 6. A comparison of the experimental (□) and theoretical (solid) pulse angle dependence of the ratio of SSFP echo to SSFP FID for 0.5 mM $MnCl_2$ solution (T_1 = 277 ms, T_2 = 21 ms, T_R = 20 ms).

transverse magnetization is strong but only short-term. At low flip angles the interchange is weaker, since weak RF pulses do little to disturb the longitudinal magnetization. They are also ineffective in disturbing any transverse magnetization which may have been generated. Thus the transverse magnetization, although weak, may remain over many repetitions.

APPENDIX

The purpose of this appendix is to integrate [15] with respect to resonance offset $\delta\omega$

$$S(t) = \frac{M_0(1 - E_1(T_R))}{p} \sin(\alpha)\left\{ E_2(t) \int_{-\infty}^{+\infty} \frac{g(\delta\omega)e^{j\delta\omega t}}{1 - (q/p)\cos(\delta\omega T_R)}\, d(\delta\omega) \right.$$
$$\left. - E_2(t + T_R) \int_{-\infty}^{+\infty} \frac{g(\delta\omega)e^{j\delta\omega(t - T_R)}}{1 - (q/p)\cos(\delta\omega T_R)}\, d(\delta\omega) \right\}. \quad [23]$$

Since $|p| > |q|$ for all α and $T_2 < T_1$ (*13*) the term $(1 - (q/p)\cos(\delta\omega T_R))^{-1}$ in [23] may be expanded as a geometrical series; therefore

$$\left(1 - \left(\frac{q}{p}\right)\cos(\delta\omega T_R)\right)^{-1} = 1 + \sum_{n=1}^{\infty} \left(\frac{q}{p}\right)^n \cos^n(\delta\omega T_R) \quad [24]$$

and since $\cos(x) = (1/2)e^{jx}(1 + e^{-2jx})$ [24] becomes

$$= 1 + \sum_{n=1}^{\infty} \left(\frac{q}{2p}\right)^n e^{(jn\delta\omega T_R)}(1 + e^{(-2j\delta\omega T_R)})^n \quad [25]$$

by applying a binomial expansion [25] becomes

$$= 1 + \sum_{n=1}^{\infty} \left(\frac{q}{2p}\right)^n \left[e^{(jn\delta\omega T_R)} + \sum_{m=1}^{n} \binom{n}{m} e^{(j(n-2m)\delta\omega T_R)} \right] \quad [26]$$

substituting [26] into [23] and noting that

$$f(t') = \int_{-\infty}^{+\infty} g(\delta\omega)e^{j\delta\omega t'}\, d(\delta\omega) \quad [27]$$

i.e., $f(t')$ is the Fourier transform of $g(\delta\omega)$. Thus [20] becomes

$$S(t) = \frac{M_0(1 - E_1(T_R))\sin(\alpha)}{p} \left\{ E_2(t) \left[f(t) \right.\right. \quad [28a]$$
$$+ \sum_{n=1}^{\infty} \left(\frac{q}{2p}\right)^n f(t + nT_R) \quad [28b]$$
$$+ \sum_{n=1}^{\infty} \left(\frac{q}{2p}\right)^n \sum_{m=1}^{n} \binom{n}{m}$$
$$\left.\left. \times f(t + (n - 2m)T_R) \right] \right. \quad [28c]$$
$$\left. - E_2(t + T_R) \left[f(t - T_R) \right. \right. \quad [28d]$$

$$+\sum_{n=1}^{\infty}\left(\frac{q}{2p}\right)^{n} f(t+(n-1)T_{\mathrm{R}}) \qquad [28e]$$

$$+\sum_{n=1}^{\infty}\left(\frac{q}{2p}\right)^{n}\sum_{m=1}^{n}\binom{n}{m}$$

$$\times f(t+(n-2m-1)T_{\mathrm{R}})\Bigg]\Bigg\}. \qquad [28f]$$

In [28a] $f(t)$ is the principal component of the SSFP FID signal, at a maximum immediately after each pulse and decaying away through each repetition interval. The term $f(t - T_{\mathrm{R}})$ in [28d] is a component of the SSFP echo signal reaching a maximum at the end of the interval when $t = T_{\mathrm{R}}$. The signals described by [28b], [28c], [28e], and [28f] represent additional contributions to [28a] and [28d] from higher-order echoes. In general the additional terms describe signals which peak at times $t = kT_{\mathrm{R}}$ (where k is any positive or negative integer). If signals from previous repetitions have no contribution in the current interval, $0 < t < T_{\mathrm{R}}$, only signals for which $k = 0$ and $k = +1$ are of interest; i.e., $f(t) \approx 0$ for $|t| > |T_{\mathrm{R}}|$. Thus [28b] gives no contribution. For [28c]

$$k = 2m - n; \qquad [29]$$

therefore $n = 2m$ for $k = 0$ and $n = 2m - 1$ for $k = 1$ and [28c] becomes

$$\sum_{m=1}^{\infty}\left(\frac{q}{2p}\right)^{2m}\binom{2m}{m}f(t)+\frac{1}{2}\sum_{m=1}^{\infty}\left(\frac{q}{2p}\right)^{2m-1}\binom{2m}{m}f(t-T_{\mathrm{R}}) \qquad [30]$$

providing contributions to both the FID and the echo components. In [28e] $n = 1$ if $k = 0$, therefore this term becomes

$$(q/2p)f(t) \qquad [31]$$

making contributions only to the FID. In [28f]

$$k = 2m - n + 1; \qquad [32]$$

therefore $n = 2m + 1$ for $k = 0$ and $n = 2m$ for $k = 1$ and [28f] becomes

$$\sum_{m=1}^{\infty}\left(\frac{q}{2p}\right)^{2m}\binom{2m}{m}f(t-T_{\mathrm{R}})+\sum_{m=1}^{\infty}\left(\frac{q}{2p}\right)^{2m+1}\binom{2m+1}{m}f(t). \qquad [33]$$

Combining [31] with [33] gives

$$\sum_{m=1}^{\infty}\left(\frac{q}{2p}\right)^{2m}\binom{2m}{m}f(t-T_{\mathrm{R}})+\frac{1}{2}\sum_{m=1}^{\infty}\left(\frac{q}{2p}\right)^{2m-1}\binom{2m}{m}f(t) \qquad [34]$$

and the NMR signal appearing between pulses is given by

$$S(t)=\frac{M_0(1-E_1(T_{\mathrm{R}}))}{p}\sin(\alpha)\times\Big\{(E_2(t)u-E_2(t+T_{\mathrm{R}})v)f(t)$$

$$-(E_2(t+T_{\mathrm{R}})u-E_2(t)v)f(t-T_{\mathrm{R}})\Big\}, \qquad [35]$$

where

$$u = 1 + \sum_{m=1}^{\infty} \left(\frac{q}{2p}\right)^{2m} \binom{2m}{m} \quad [36]$$

$$v = \frac{1}{2} \sum_{m=1}^{\infty} \left(\frac{q}{2p}\right)^{2m-1} \binom{2m}{m}. \quad [37]$$

The FID signal occurring immediately after each RF pulse, at $t = 0$, is given by

$$S_{\text{fid}} = \frac{M_0(1 - E_1(T_R))}{p} \sin(\alpha)(u - E_2(T_R)v) \quad [38]$$

and the echo signal occurring at the end of each repetition, at $t = T_R$, is given by

$$S_{\text{echo}} = \frac{M_0(1 - E_1(T_R))}{p} \sin(\alpha)(E_2(2T_R)u - E_2(T_R)v). \quad [39]$$

ACKNOWLEDGMENTS

This work was started in the Advanced Development Group of Picker International Limited, Wembley, England. The experimental data presented in this paper were acquired at the Max-Planck Institut für biophysikalische Chemie, Göttingen, Federal Republic of Germany. The theoretical data were calculated using the facilities of the Gesellschaft für wissenschaftliche Datenverarbeitung, Göttingen.

The author thanks Rob Dickinson, Martyn Paley, and Chris Randell at Picker, and also Jens Frahm, Wolfgang Hänicke, and Dietmar Merboldt for many useful discussions.

REFERENCES

1. A. HAASE, J. FRAHM, D. MATTHAEI, W. HÄNICKE, AND K. D. MERBOLDT, *J. Magn. Reson.* **67,** 256 (1986).
2. M. L. GYNGELL, G. L. NAYLER, N. PALMER, AND M. PALEY, *Magn. Reson. Imaging* **4,** 101 (1986).
3. F. W. WEHRLI, "Introduction to Fast-Scan Magnetic Resonance," General Electric, 1985.
4. P. VAN DER MEULEN, J. P. GROEN, AND J. J. M. CUPPEN, *Magn. Reson. Imaging* **3,** 297 (1985).
5. M. L. GYNGELL, *Magn. Reson. Imaging* **6,** 415 (1988).
6. R. C. HAWKES AND S. PATZ, *Magn. Reson. Med.* **4,** 9 (1987).
7. R. B. BUXTON, R. R. EDELMAN, B. R. ROSEN, G. L. WISMAR, AND T. J. BRADY, *J. Comput. Assist. Tomogr.* **11,** 7 (1987).
8. P. VAN DER MEULEN, *Magn. Reson. Imaging* **6,** 355 (1988).
9. Y. ZUR, S. STOKAR, AND P. BENDEL, *Magn. Reson. Med.* **6,** 175 (1988).
10. H. Y. CARR, *Phys. Rev.* **112,** 1693 (1958).
11. W. S. HINSHAW, *J. Appl. Phys.* **47,** 3709 (1976).
12. K. N. SCOTT, H. R. BROOKER, J. R. FITZSIMMONS, H. F. BENNETT, AND R. C. MICK, *J. Magn. Reson.* **50,** 339 (1982).
13. M. L. GYNGELL, Ph.D. thesis, Nottingham (1987).
14. R. KAISER, E. BARTHOLDI, AND R. R. ERNST, *J. Chem. Phys.* **60,** 2966 (1974).
15. J. HENNIG, "Sixth Annual Meeting of the Society for Magnetic Resonance in Medicine, New York, 1987, Book of Abstracts," p. 231.
16. S. MATSUI, K. KURODA, AND H. KOHNO, *J. Magn. Reson.* **62,** 12 (1985).